Ecological & Sustainable Materials Connect
ISSN: 3136-344X
2026, Article ID. 2026.0010, Cite as: https://doi.org/10.69709/ESM.2026.111212

SCIFINITI PUBLISHING

Research Article

OPEN ACCESS

Prediction of Natural Fiber Composite Mechanical Properties with a Multilayer Artificial Neural Network

Nashat Nawafleh[✉,1,2,*], **Faris M. AL-Oqla**[✉,1]

[1] Department of Mechanical Engineering, Faculty of Engineering, The Hashemite University, P.O. Box 330127, Zarqa 13133, Jordan
[2] Department of Engineering and Information Technology, Technical College, The Hashemite University, P.O. Box 330127, Zarqa 13133, Jordan

Article History
Received: April 25, 2026 Accepted: October 04, 2026

Abstract
Owing to their environmental and cost advantages, natural fiber–reinforced composites are currently employed in a wide range of applications. However, these composites pose production challenges, such as poor adhesion between the reinforcement and the matrix. Consequently, a comprehensive artificial neural network (ANN) framework is adopted to predict the mechanical properties of green composites, particularly ultimate tensile strength (UTS) and Young's modulus, thereby reducing the burden of experimental work. Because the mechanical properties of biofibers depend on several key influencing parameters that may differ considerably from one fiber to another, predicting biofiber properties is highly complex. Therefore, this paper employs an ANN framework with nonlinear activation functions to predict the mechanical properties of natural fibers—specifically UTS and Young's modulus—based on cellulose content, microfibrillar angle, and fiber diameter. The developed ANN system comprises three model architectures for predicting the mechanical properties of natural fiber composites, among which the 3-6-12-18-2 model yielded the most accurate predictions. The results show that the ANN model can enhance the scientific evaluation of green fibers and help determine their suitability as a replacement material for effective green product manufacturing in future eco-friendly industries.

ACCEPTED ARTICLE

Keywords:
green composite materials; natural fibers; artificial neural network; cellulose content; mechanical performance

1. Introduction

As the traditional take-make-dispose economic model transitions into a circular, bio-based one, natural fiber–reinforced polymer (NFRP) materials have gained prominence in materials development. Owing to increasingly stringent environmental regulations and recurrent, sharp spikes in oil prices, the automotive, construction, and aerospace sectors are actively seeking to adopt "green" composites as load-bearing materials [1,2]. Because the stiffness of these composite materials is comparable to that of traditional fibers in terms of both force per gram and specific volume ratio, the general principles governing wood-fiber reinforcement apply broadly, though not exactly, apply. Fiber properties significantly influence the overall mechanical performance of green composites; for example, increasing the cellulose content of the reinforcing fiber can improve mechanical and thermal stability. Similarly, lower microfibrillar angles yield stiffer composites, whereas higher angles yield more compliant ones [3–6]. In recent years, as environmental concerns have grown, increasing attention has been paid to sources of cellulosic fiber, which are numerous and include kenaf, cotton, jute, and hemp. These fibers are used in a wide range of products and composites. Notably, the value of these fibers lies not so much in their use for pulp or paper production as in their subsequent applications, which

* **Corresponding Author:**
Nashat Nawafleh, Department of Mechanical Engineering, Faculty of Engineering, The Hashemite University, P.O. Box 330127, Zarqa 13133, Jordan;
Department of Engineering and Information Technology, Technical College, The Hashemite University, P.O. Box 330127, Zarqa 13133, Jordan,
nashatm@hu.edu.jo

© 2026 Copyright by the Authors.
Licensed as an open access article using a CC BY 4.0 license.

2026, Vol. 1, Article ID. 2026.0010
https://doi.org/10.69709/ESM.2026.111212

invariably involve downcycling. In particular, their use as reinforcements in polymer composites has attracted considerable interest [7–11]. The results in Table 1 indicate that the mechanical properties of natural fibers change when their cellulose content decreases, their microfibrillar angle varies, or their diameter increases relative to those of commonly used fibers [12–19].

Table 1: Mechanical properties of natural fibers reported in several experimental studies.

Fiber Type	Microfibrillar Angle (deg)	Cellulose Content (wt%)	Diameter (μm)	Ultimate Tensile Strength (MPa)	Young's Modulus (GPa)
Cotton	32–35	82.7–95	10–45	400–980	6.2–20
Jute	8	61–71.5	20–200	320–800	8–78
Kenaf	7.1–15	45–57	65.2–77	400–938	61.4–128
Bamboo	8–11	35–74	14.0–88	270–862	17–89
Sisal	10–22	66–78	8–200	363–700	9–38

However, the mechanical integrity of green composites arises from a complex interplay of variables that is extremely difficult to predict. The fundamental problem remains the poor interfacial adhesion between hydrophilic biofibers and typically hydrophobic resin matrices. Because stress transfer is impeded, premature failure occurs [20,21]. Previous authors have highlighted the limitations of analytical modeling, and artificial neural networks (ANNs) have emerged as a promising approach in predictive materials science to overcome them. Modeled on the way the brain processes information through biological neurons, ANNs can learn hidden relationships within experimental data without requiring explicit governing physical equations. This capability is especially beneficial for understanding green composites, as the effect of chemical processing on ultimate tensile strength may be nonlinear and may even be linked to fiber aspect ratio. As in biological neural networks, each artificial neuron in an ANN is linked to all others [22,23]. The neuron's output is computed as a nonlinear function of the sum of its inputs, and these summands are represented by real numbers [24,25]. Indeed, ANNs are widely used in various disciplines, such as structural engineering, concrete expansion prediction, resource engineering, robotics, and composite materials [26–28]. ANNs can handle high-dimensional datasets and generate highly correlated predictive maps using various architectures, such as the multilayer perceptron (MLP). Although previous work has covered broad topics such as the general application of machine learning to composites, an important question remains open: how to develop more specific models that improve the selection of natural fibers for biomaterials in green systems. This study addresses this question by developing an integrated ANN framework trained on a large array of experimental datasets. It not only examines the optimization of the hidden-layer structure to minimize the mean squared error (MSE) but also evaluates the predictive capability of the multilayer network across key fiber parameters to establish accurate design maps for green composite materials.

ACCEPTED ARTICLE

2. Methodology

An artificial neural network (ANN) typically comprises three main components: an input layer, an output layer, and one or more hidden layers in between. The process begins with the input layer receiving data from outside the system. These data are then transformed by the hidden layers before the final output is generated. The neuron is the basic building block of this system, as shown in Figure 1. Each neuron receives inputs from the preceding nodes, scales them by specific weights, sums them, and applies an activation function to generate a signal for the next layer.

By arranging neurons in multiple layers, an artificial neural network becomes capable of performing extremely complex operations. For this purpose, three prediction models were developed in this study using the MATLAB environment to simulate tensile stress and Young's modulus. The key distinguishing feature of these models is the increasing number of hidden layers and neurons in each layer. The three input parameters common to all models are the cellulose content, the microfibrillar angle (in degrees), and the diameter (in micrometers). The models output Young's modulus and ultimate tensile strength. Accordingly, Model I has a single hidden layer with six neurons, whereas Model II has two hidden layers containing six and twelve neurons, respectively. To determine whether the prediction of mechanical performance improves further, Model III was created with three hidden layers containing six, twelve, and eighteen neurons, respectively. Furthermore, the log-sigmoid transfer function, which is well suited to linking the hidden and output layers, transmits each neuronal output signal to the subse-

2026, Vol. 1, Article ID. 2026.0010
https://doi.org/10.69709/ESM.2026.111212

quent layer in the simulation (Figure 2). Table 2 summarizes the models used in this work, and Table 3 details the hyperparameters and all training settings.

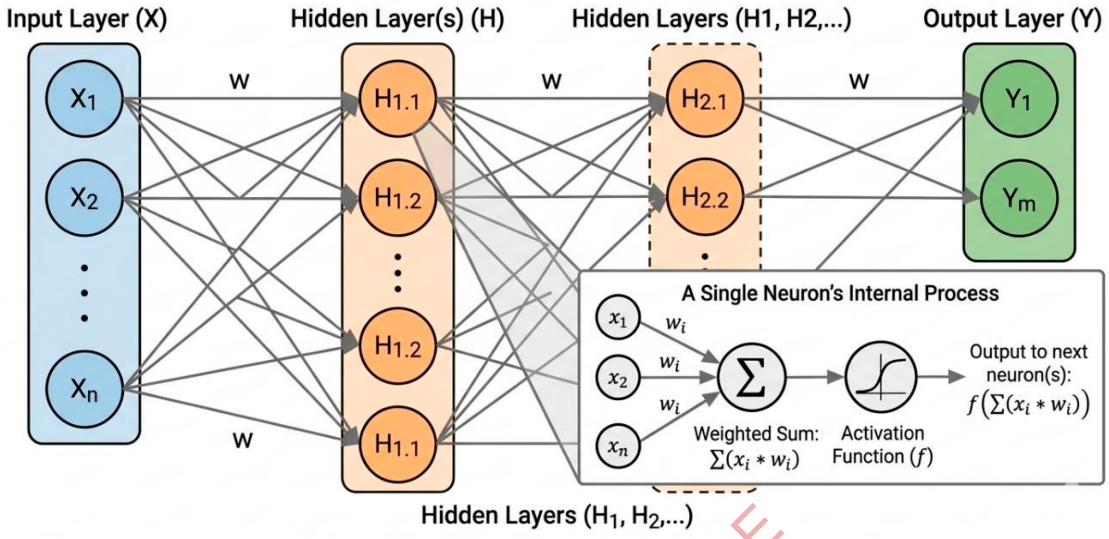

Figure 1: The multilayered hierarchy of an ANN and the internal process of a neuron, including weighted summation and application of the activation function.

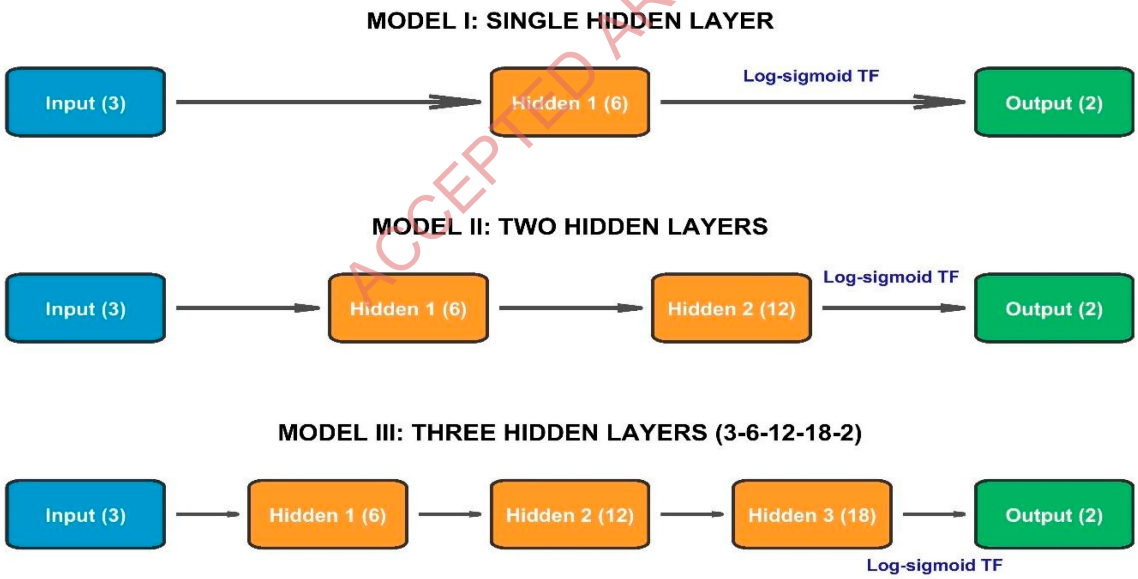

Figure 2: Schematic progression of artificial neural network (ANN) architectures (Models I–III) simulated in the MATLAB environment.

Table 2: Comparison of ANN architectures.

Model Type	Hidden Layers	Neurons in Each Hidden Layer	Transfer Function Type
Model I	1	6	Log-sigmoid
Model II	2	6, 12	Log-sigmoid
Model III	3	6, 12, 18	Log-sigmoid

ACCEPTED ARTICLE

Table 3: Hyperparameters and settings for the artificial neural network (ANN) model.

Parameter	Value/Configuration
Optimization Algorithm	Levenberg-Marquardt (trainlm)
Weight Initialization	Uniform weight distribution
Initial Learning Rate	0.001
Performance Goal (MSE)	10^{-5}
Minimum Gradient	10^{-7}
Validation Checks	6 consecutive epochs
Maximum Training Epochs	380

Equation (1) gives the mathematical expression of the log-sigmoid function:

$$logsig(j) = \frac{1}{1 + e^{-j}} \tag{1}$$

The log-sigmoid is a well-known transfer function in multilayer neural networks trained using the backpropagation technique. This function produces outputs between 0 and 1 as the net input to the neuron ranges from negative to positive infinity. In this study, the following approach is used: the weights between neurons are initially assigned random values. The networks are then trained on the data so that input values are mapped to outputs.

3. Results and Discussion

The developed ANN models were trained and tested using a dataset comprising N = 300 discrete experimental data points. The database was compiled from extensive experimental research and published literature on natural fiber characterization [12–17]. A rigorous discretization of the stated experimental ranges for the input parameters (cellulose content, microfibrillar angle, and diameter) and the outputs (Table 1) was performed to establish a one-to-one correspondence between each synthetic input combination and its target. The dataset includes five major natural lignocellulosic fibers: cotton, jute, kenaf, bamboo, and sisal. Each data point in this dataset is a discrete vector of three physical input features, namely cellulose content (wt%), microfibrillar angle (deg), and fiber diameter (μm), which are directly mapped to the corresponding experimental output properties: ultimate tensile strength (UTS, MPa) and Young's modulus (YM, GPa). The wide property ranges, representative of the inherent variability of the sample set, are summarized in Table 1. Before training, the 300 dataset samples were randomly split into two independent subsets: 70% (n = 210 samples) for model training and 30% (n = 90 samples) for model testing and validation to estimate generalization capability.

The process began with the method producing global output data, after which the networks were trained on the input data. Backpropagation gradient descent formed the basis of the training process owing to its simplicity and efficacy, even in multilayer networks. First, the algorithm received the input training values, and then the network computed its outputs. This division into phases facilitates understanding of the backpropagation technique. The second step was to determine the extent to which the calculated results deviate from the target values. Third, the error was propagated backward to adjust the layer weights.

Here, the ANN is applied to analyze the mechanical properties of fiber materials from experimental data. The objective is to compare the model predictions with the experimental results for average tensile stress and Young's modulus. Tables 4–6 compare the experimental values with the ANN-predicted tensile stress (TS) and Young's modulus (YM) for Models I, II, and III, respectively.

ACCEPTED ARTICLE

Table 4: Comparison of experimental and ANN-predicted mechanical properties of various natural fibers: Model I.

Fiber Type	Microfibrillar Angle (deg)	Cellulose Content (wt%)	Diameter (μm)	TS (MPa)	Predicted TS (MPa)	YM (GPa)	Predicted YM (GPa)
Cotton	32–35	82.7–95	10–45	400–980	710.2–1300.1	6.2–20	11.2–40.5
Jute	8	61–71.5	20–200	320–800	690.7–1513.2	8–78	16.9–129.1
Kenaf	7.1–15	45–57	65.2–77	400–938	824–1872.1	61.4–128	100.7–188.4
Bamboo	8–11	35–74	14.0–88	270–862	500.9–1269.3	17–89	44.6–125.8
Sisal	10–22	66–78	8–200	363–700	972.9–1108.2	9–38	20.7–68.3

2026, Vol. 1, Article ID. 2026.0010
https://doi.org/10.69709/ESM.2026.111212

Table 5: Comparison of experimental and ANN-predicted mechanical properties of various natural fibers: Model II.

Fiber Type	Microfibrillar Angle (deg)	Cellulose Content (wt%)	Diameter (μm)	TS (MPa)	Predicted TS (MPa)	YM (GPa)	Predicted YM (GPa)
Cotton	32–35	82.7–95	10–45	400–980	459.1–1102.4	6.2–20	8.8–30.8
Jute	8	61–71.5	20–200	320–800	390.7–988.5	8–78	11.5–91.6
Kenaf	7.1–15	45–57	65.2–77	400–938	483.4–1010.2	61.4–128	77.8–150.6
Bamboo	8–11	35–74	14.0–88	270–862	400.9–999.6	17–89	40.8–100.1
Sisal	10–22	66–78	8–200	363–700	589.1–910.5	9–38	14.2–51.7

Table 6: Comparison of experimental and ANN-predicted mechanical properties of various natural fibers: Model III.

Fiber Type	Microfibrillar Angle (deg)	Cellulose Content (wt%)	Diameter (μm)	TS (MPa)	Predicted TS (MPa)	YM (GPa)	Predicted YM (GPa)
Cotton	32–35	82.7–95	10–45	400–980	408.9–1005.6	6.2–20	6.5–21.3
Jute	8	61–71.5	20–200	320–800	315.2–816.8	8–78	8.2–74.7
Kenaf	7.1–15	45–57	65.2–77	400–938	388.6–970.4	61.4–128	57.7–134.5
Bamboo	8–11	35–74	14.0–88	270–862	262.9–861.3	17–89	18.1–90.1
Sisal	10–22	66–78	8–200	363–700	370.5–701.2	9–38	9.8–42.8

Table 4 shows that Model I (a single hidden layer with six neurons) has significant predictive limitations and substantially overpredicts at the upper bound. For example, the measured tensile strength of jute fibers is 320–800 MPa, but Model I predicts 690.7–1513.2 MPa, a clear overprediction at the upper bound. This mismatch highlights the intrinsic weakness of shallow neural network topologies in mapping complex, nonlinear biocomposite characteristics. A network with only one hidden layer lacks the high-dimensional mapping capacity to adequately resolve the intricate interaction of low microfibrillar angles and large differences in fiber diameter. Consequently, the shallow network exhibits large variance and unconstrained gradient propagation, resulting in unrealistic extrapolation.

This limitation explains why deeper, multilayered architectures (Model III) are essential to constrain predictions within physical limits. These results clearly demonstrate that Model III achieves the highest accuracy among the three models, with ANN predictions very close to the experimental data. This improvement is attributable to the use of multiple hidden layers with a larger number of neurons. Figures 3 and 4 present the relative errors of Model III, which show only small deviations.

ACCEPTED ARTICLE

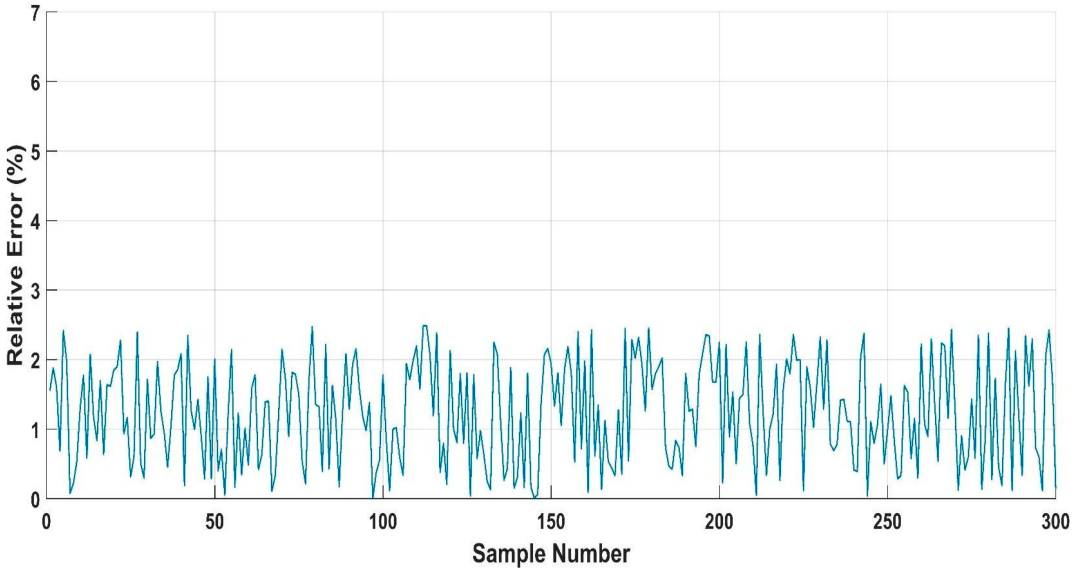

Figure 3: Relative error of ANN tensile stress predictions—Model III.

2026, Vol. 1, Article ID. 2026.0010
https://doi.org/10.69709/ESM.2026.111212

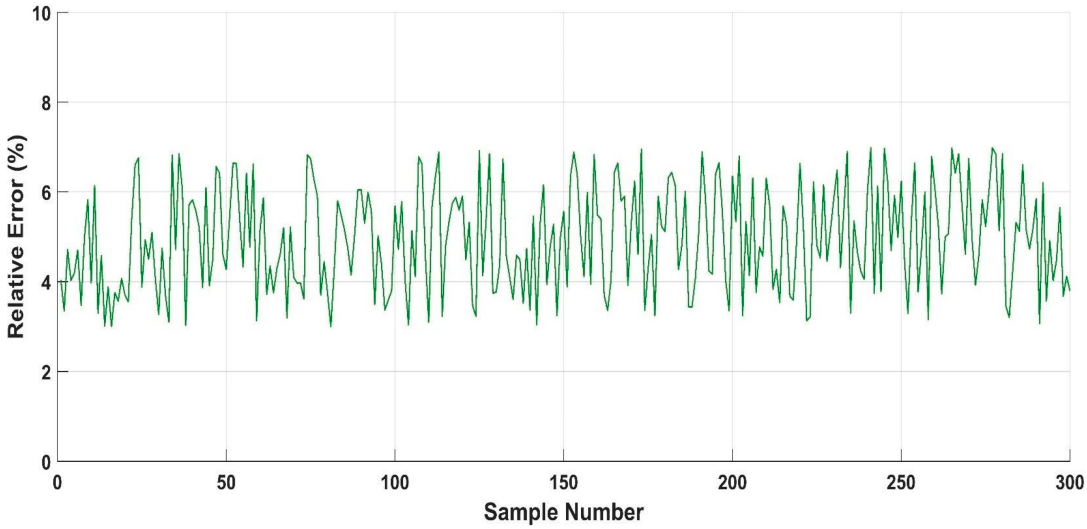

Figure 4: Relative error of ANN Young's modulus predictions—Model III.

Tensile strength is the target variable, i.e., output from the model for the columns of the data set against many permutations of inputs, which is seen in Figures 5–7. The predicted outcomes are clearly very close to the actual experimental outcomes, thereby validating the predictive models developed in this work.

Similarly, Figures 8–10 show that the ANN-predicted outcomes for Young's modulus are very close to the actual experimental outcomes.

The performance of Model III was further validated through statistical analysis, which yielded mean absolute percentage error (MAPE) values of 5.28% and 3.61% for tensile strength and Young's modulus, respectively, confirming that increasing the number of hidden layers enhances the accuracy of the predictive model. MAPE is defined as:

$$MAPE = \frac{1}{Q}\sum_{K=1}^{Q}\frac{|\varepsilon_{p,Q} - \varepsilon_{exp,Q}|}{\Omega_{exp,Q}} \quad (2)$$

where Q is the number of samples, ε_p is the predicted value of the mechanical property, and ε_{exp} is its measured value.

ACCEPTED ARTICLE

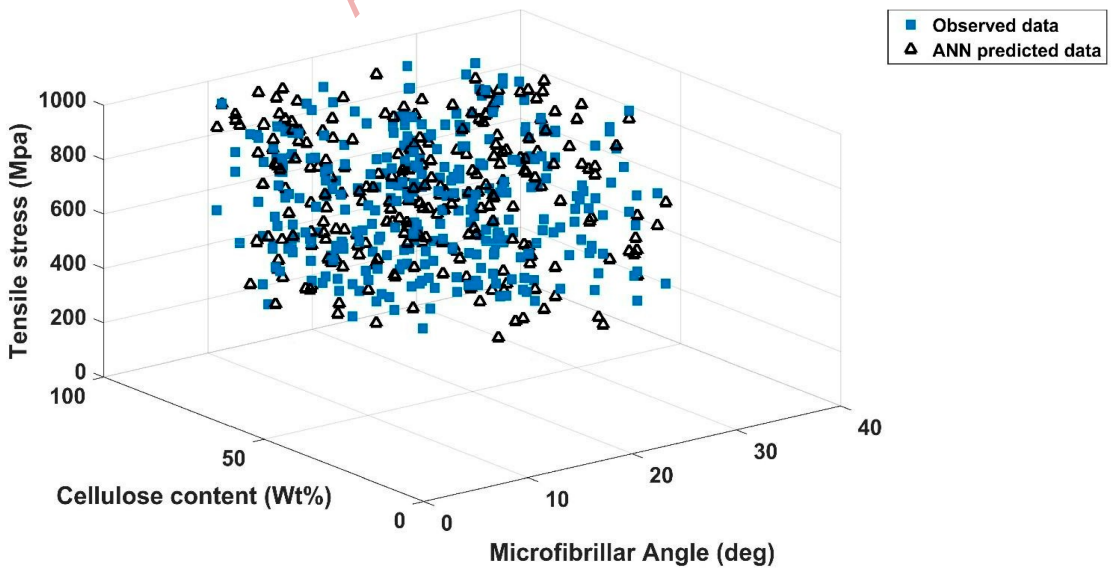

Figure 5: 3D plot showing the relationship between two input predictors, microfibrillar angle and cellulose content, and the tensile strength output.

2026, Vol. 1, Article ID. 2026.0010
https://doi.org/10.69709/ESM.2026.111212

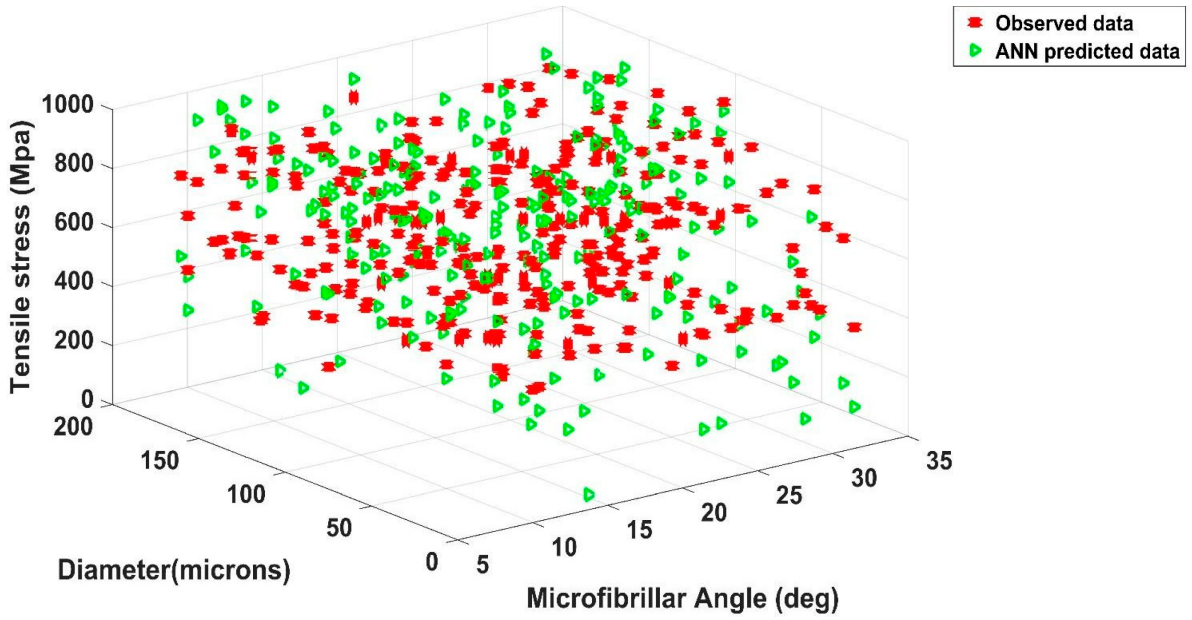

Figure 6: 3D plot showing the relationship between two input predictors, microfibrillar angle and fiber diameter, and the tensile strength output.

ACCEPTED ARTICLE

Furthermore, to verify the accuracy of Model III, 10-fold cross-validation (K = 10) was applied across all three model architectures. Model III consistently demonstrated high stability across folds, with mean R^2 values of 0.92 for UTS and 0.94 for Young's modulus, confirming strong generalization capability without overfitting, as illustrated in Table 7. The coefficient of determination was used to validate the models by comparing the predicted and experimental values, as illustrated in Figure 11. The closer the coefficient of determination is to one, the better the training of the model and the more accurate its predictions.

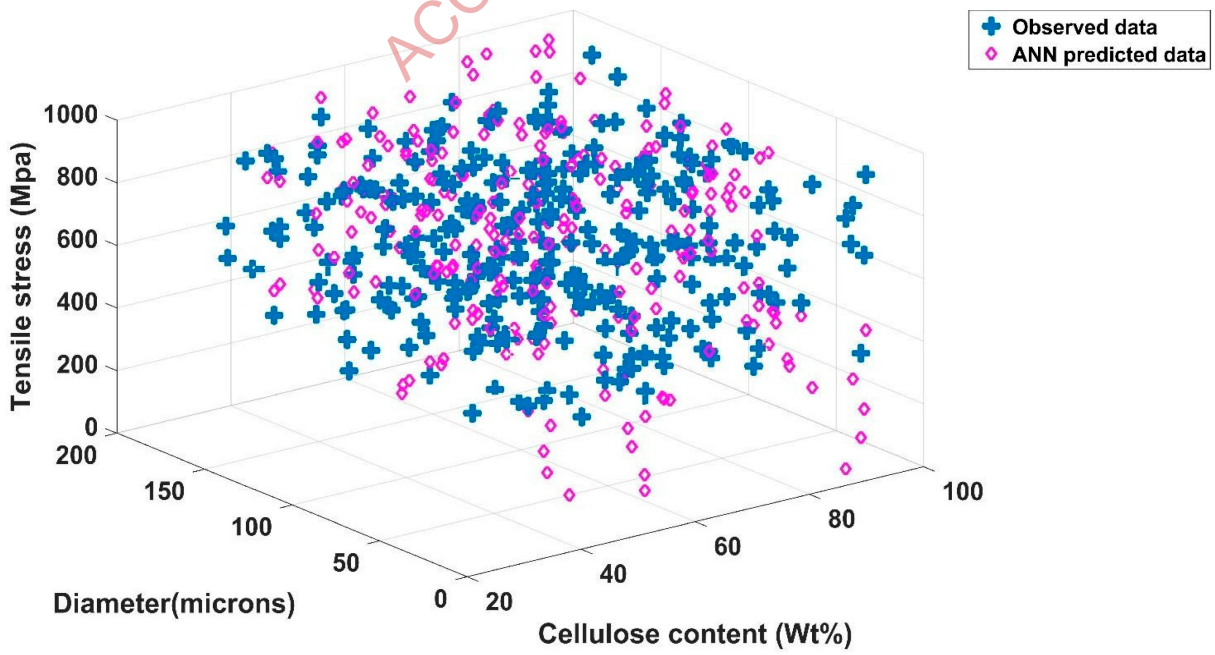

Figure 7: 3D plot showing the relationship between two input predictors, fiber diameter and cellulose content, and the tensile strength output.

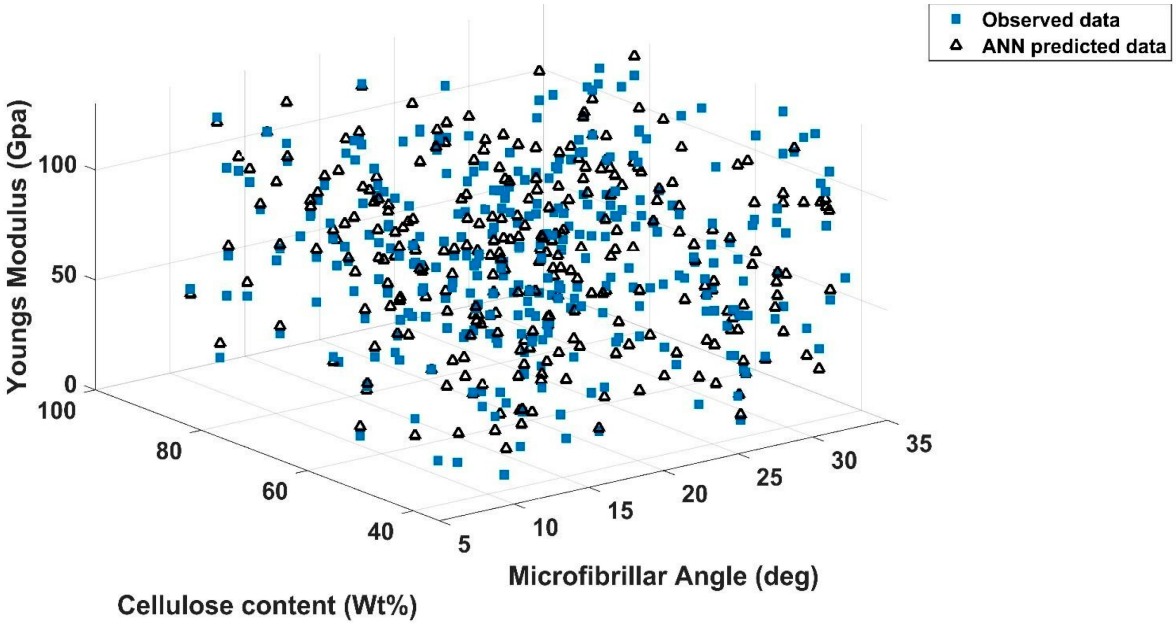

Figure 8: 3D plot showing the relationship between two input predictors, microfibrillar angle and cellulose content, and the Young's modulus output.

ACCEPTED ARTICLE

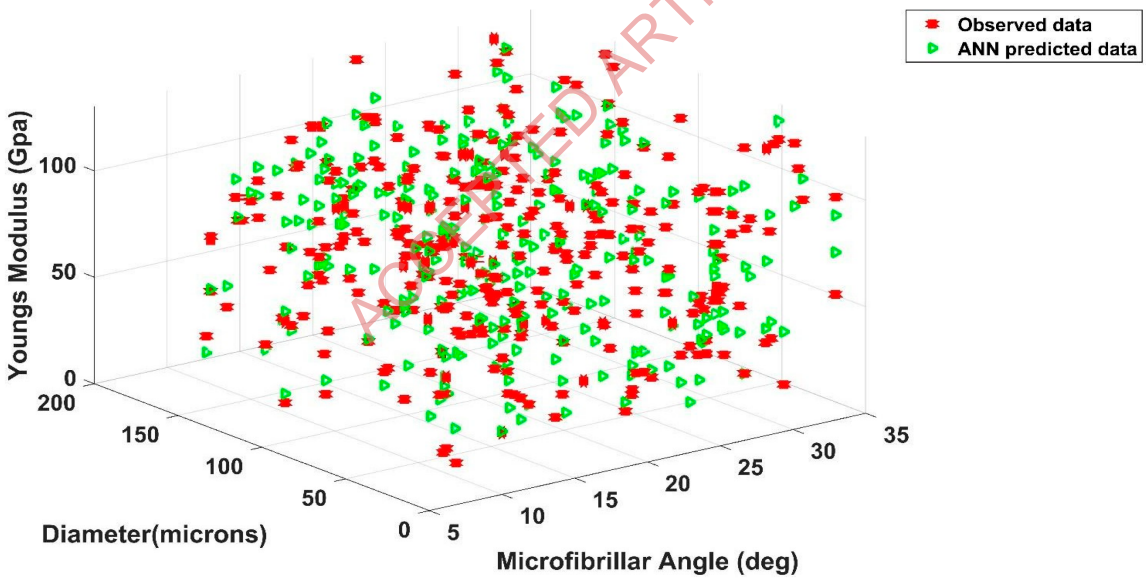

Figure 9: 3D plot showing the relationship between two input predictors, microfibrillar angle and fiber diameter, and the Young's modulus output.

Table 7: Performance evaluation of neural network models for predicting tensile stress and Young's modulus across different architectures.

System Model	Hidden Layers	Neurons	Tensile Stress R^2 (Mean ± SD)	Tensile Stress MAPE (%) (Mean ± SD)	Young's Modulus R^2 (Mean ± SD)	Young's Modulus MAPE (%) (Mean ± SD)
Model I	1	6	0.78 ± 0.04	14.21 ± 1.85	0.81 ± 0.05	11.45 ± 1.62
Model II	2	6, 12	0.86 ± 0.03	8.74 ± 1.12	0.88 ± 0.03	7.10 ± 0.95
Model III	3	6, 12, 18	0.92 ± 0.02	5.28 ± 0.45	0.94 ± 0.015	3.61 ± 0.38

2026, Vol. 1, Article ID. 2026.0010
https://doi.org/10.69709/ESM.2026.111212

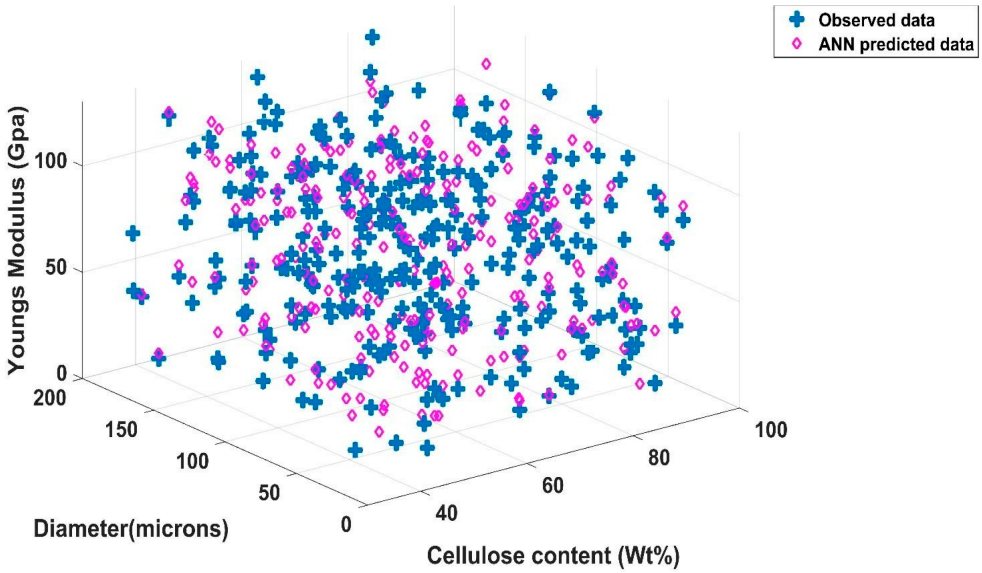

Figure 10: 3D plot showing the relationship between two input predictors, fiber diameter and cellulose content, and the Young's modulus output.

ACCEPTED ARTICLE

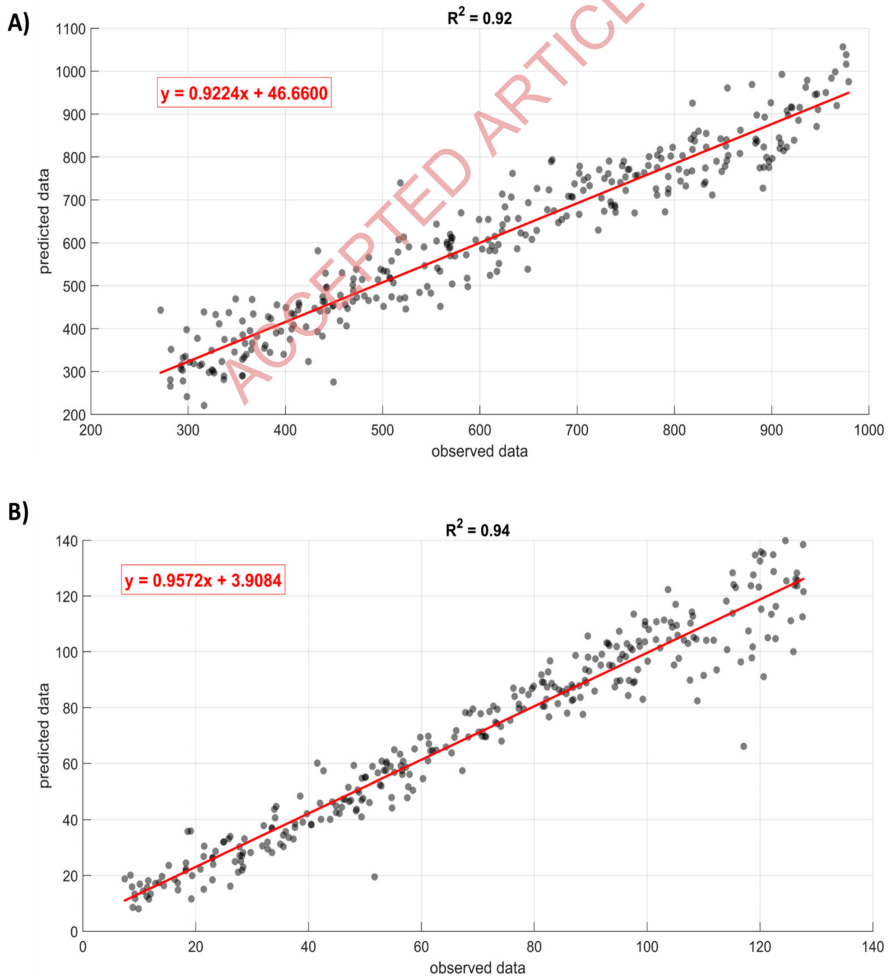

Figure 11: R-squared values for Model III: (**A**) tensile stress and (**B**) Young's modulus.

The correlation coefficient is given by:

$$R^2 = 1 - \frac{\sum_{K=1}^{Q} \left(\varepsilon_{exp,Q} - \varepsilon_{p,Q}\right)^2}{\sum_{K=1}^{Q} \left(\varepsilon_{exp,Q} - \varepsilon_{m,Q}\right)^2} \quad (3)$$

Here, $\varepsilon_{m,Q}$ represents the arithmetic mean of all actual experimental values across the dataset.

4. Conclusions

This study successfully developed an approach to analyze and predict the behavior of natural fiber–reinforced polymers. It employs ANNs to overcome the limitations of conventional linear models in composites research. The ANN structure demonstrated a strong ability to map nonlinear interactions among fiber properties, such as microfibrillar angle and cellulose content. Furthermore, the optimized hidden-layer structure minimized the mean squared error (MSE). This enables reliable prediction of tensile strength and Young's modulus in different types of natural fibers, with a high level of agreement between the experimental mechanical characteristics and the model predictions. Ultimately, the application of machine learning to biocomposites can help natural fiber–reinforced composites become competitive with those reinforced by traditional synthetic fibers. This aligns with the current need for solutions that combine high performance with environmental responsibility. Moreover, establishing this accurate forward prediction model provides a foundational framework that can support future optimization algorithms for material selection, thereby reducing reliance on empirical testing in green composite development.

List of Abbreviations

ANN	Artificial Neural Network
GPa	Gigapascal
MAPE	Mean Absolute Percentage Error
MLP	Multilayer Perceptron
MPa	Megapascal
μm	Micrometer (Micron)
MSE	Mean Squared Error
NFRP	Natural Fiber-Reinforced Polymer
SD	Standard Deviation
TS	Tensile Stress/Tensile Strength
UTS	Ultimate Tensile Strength
YM	Young's Modulus

Author Contributions

Both authors contributed equally to the conceptualization, methodology, software, formal analysis, data curation, investigation, writing—original draft, writing—review and editing, visualization, and supervision. The authors have read and agreed to the published version of the manuscript.

Availability of Data and Materials

The dataset used in this study was compiled from previously published literature (see references). Summary data are presented in Table 1, Table 4, Table 5, Table 6 and Table 7. The full raw dataset is available from the corresponding author upon reasonable request.

Conflicts of Interest

The authors declare no conflicts of interest.

Funding

The study did not receive any external funding and was conducted using only institutional resources.

Acknowledgments

None declared.

AI Declaration

The authors confirm that no artificial intelligence (AI) tools technologies were used in the writing, editing, analysis, or preparation of this manuscript. All content was produced solely by the authors, who take full responsibility for the accuracy, originality, integrity, and scientific content of the manuscript.

References

[1] Masseteau, B.; Michaud, F.; Irle, M.; Roy, A.; Alise, G. An Evaluation of the Effects of Moisture Content on the Modulus of Elasticity of a Unidirectional Flax Fiber Composite. *Compos. Part A Appl. Sci. Manuf.* **2014**, *60*, 32–37. [CrossRef]

[2] Thakur, V.; Singha, A.; Thakur, M. Biopolymers Based Green Composites: Mechanical, Thermal and Physico-Chemical Characterization. *J. Polym. Environ.* **2012**, *20*, 412–421. [CrossRef]

[3] Patil, N.V.; Rahman, M.M.; Netravali, A.N. "Green" Composites Using Bioresins from Agro-Wastes and Modified Sisal Fibers. *Polym. Compos.* **2019**, *40*, 99–108. [CrossRef]

[4] Khalil, H.A.; Bhat, A.; Yusra, A.I. Green Composites from Sustainable Cellulose Nanofibrils: A Review. *Carbohydr. Polym.* **2012**, *87*, 963–979. [CrossRef]

[5] Dun, M.; Hao, J.; Wang, W.; Wang, G.; Cheng, H. Sisal Fiber Reinforced High Density Polyethylene Pre-Preg for Potential Application in Filament Wind-

ACCEPTED ARTICLE

ing. *Compos. Part B Eng.* **2019**, *159*, 369–377. [CrossRef]

[6] Dalmis, R.; Kilic, G.B.; Seki, Y.; Koktas, S.; Keskin, O.Y. Characterization of a New Natural Cellulose Based Fiber from Hierochloe Odarata. *Cellulose* **2020**, *27*, 127–139. [CrossRef]

[7] Thakur, V.K.; Thakur, M.K. Processing and Characterization of Natural Cellulose Fibers/Thermoset Polymer Composites. *Carbohydr. Polym.* **2014**, *109*, 102–117. [CrossRef] [PubMed]

[8] Reddy, N.; Yang, Y. Properties and Potential Applications of Natural Cellulose Fibers from the Bark of Cotton Stalks. *Bioresour. Technol.* **2009**, *100*, 3563–3569. [CrossRef] [PubMed]

[9] Asyraf, M.R.M.; Rafidah, M.; Azrina, A.; Razman, M.R. Dynamic Mechanical Behaviour of Kenaf Cellulosic Fibre Biocomposites: A Comprehensive Review on Chemical Treatments. *Cellulose* **2021**, *28*, 2675–2695. [CrossRef]

[10] Reddy, N.; Yang, Y. Properties and Potential Applications of Natural Cellulose Fibers from Cornhusks. *Green Chem.* **2005**, *7*, 190–195. [CrossRef]

[11] Wang, W.-M.; Cai, Z.-S.; Yu, J.-Y.; Xia, Z.-P. Changes in Composition, Structure, and Properties of Jute Fibers After Chemical Treatments. *Fibers Polym.* **2009**, *10*, 776–780. [CrossRef]

[12] Al-Shrida, M.A.M.; Hayajneh, M.T.; AL-Oqla, F.M. Modeling and Investigation of the Influential Reinforcement Parameters on the Strength of Polypropylene Lignocellulosic Fiber Composites Using Analysis of Variances and Box-Cox Transformation Technique. *Mater. Res.* **2023**, *26*, e20220386. [CrossRef]

[13] AL-Oqla, F.M.; Al-Jarrah, R. A Novel Adaptive Neuro-Fuzzy Inference System Model to Predict the Intrinsic Mechanical Properties of Various Cellulosic Fibers for Better Green Composites. *Cellulose* **2021**, *28*, 8541–8552. [CrossRef]

[14] Hayajneh, M.T.; Mu'ayyad, M.; AL-Oqla, F.M. Mechanical, Thermal, and Tribological Characterization of Bio-Polymeric Composites: A Comprehensive Review. *e-Polymers* **2022**, *22*, 641–663. [CrossRef]

[15] AL-Oqla, F.M.; Sapuan, S. Investigating the Inherent Characteristic/Performance Deterioration Interactions of Natural Fibers in Bio-Composites for Better Utilization of Resources. *J. Polym. Environ.* **2018**, *26*, 1290–1296. [CrossRef]

[16] AL-Oqla, F.M.; Sapuan, S.M.; Ishak, M.R.; Nuraini, A.A. Predicting the Potential of Agro Waste Fibers for Sustainable Automotive Industry Using a Decision Making Model. *Comput. Electron. Agric.* **2015**, *113*, 116–127. [CrossRef]

[17] AL-Oqla, F.M.; Sapuan, S.M. Natural Fiber Reinforced Polymer Composites in Industrial Applications: Feasibility of Date Palm Fibers for Sustainable Automotive Industry. *J. Clean. Prod.* **2014**, *66*, 347–354. [CrossRef]

[18] Karimah, A.; Ridho, M.R.; Munawar, S.S.; Adi, D.S.; Ismadi; Damayanti, R.; Subiyanto, B.; Fatriasari, W.; Fudholi, A. A Review on Natural Fibers for Development of Eco-Friendly Bio-Composite: Characteristics, and Utilizations. *J. Mater. Res. Technol.* **2021**, *13*, 2442–2458. [CrossRef]

[19] Zwawi, M. A Review on Natural Fiber Bio-Composites, Surface Modifications and Applications. *Molecules* **2021**, *26*, 404. [CrossRef] [PubMed]

[20] Dashtizadeh, Z.; Khalina, A.; Cardona, F.; Lee, C.H. Mechanical Characteristics of Green Composites of Short Kenaf Bast Fiber Reinforced in Cardanol. *Proc. Adv. Mater. Sci. Eng.* **2019**, *2019*, 8645429. [CrossRef]

[21] Hussain, M.; Levacher, D.; Leblanc, N.; Zmamou, H.; Djeran-Maigre, I.; Razakamanantsoa, A.; Saouti, L. Analysis of Physical and Mechanical Characteristics of Tropical Natural Fibers for Their Use in Civil Engineering Applications. *J. Nat. Fibers* **2023**, *20*, 2164104. [CrossRef]

[22] Gupta, N. Artificial Neural Network. *Netw. Complex Syst.* **2013**, *3*, 24–28.

[23] Kukreja, H. An Introduction to Artificial Neural Network. *Int. J. Adv. Res. Innov. Ideas. Educ.* **2016**, *1*, 27–30.

[24] Jiang, Z.; Zhang, Z.; Friedrich, K. Prediction on Wear Properties of Polymer Composites with Artificial Neural Networks. *Compos. Sci. Technol.* **2007**, *67*, 168–176. [CrossRef]

[25] Kazi, M.-K.; Eljack, F.; Mahdi, E. Optimal Filler Content for Cotton Fiber/PP Composite Based on Mechanical Properties Using Artificial Neural Network. *Compos. Struct.* **2020**, *251*, 112654. [CrossRef]

[26] Liu, X. A Review of Artificial Neural Networks in the Constitutive Modeling of Composite Materials. *Compos. Part B Eng.* **2021**, *224*, 109152. [CrossRef]

[27] Sabiston, T.; Inal, K.; Lee-Sullivan, P. Application of Artificial Neural Networks to Predict Fibre Orientation in Long Fibre Compression Moulded Composite Materials. *Compos. Sci. Technol.* **2020**, *190*, 108034. [CrossRef]

[28] Torregrosa, A.J.; Gil, A.; Quintero, P.; Cremades, A. A Reduced Order Model Based on Artificial Neural Networks for Nonlinear Aeroelastic Phenomena and Application to Composite Material Beams. *Compos. Struct.* **2022**, *295*, 115845. [CrossRef]

ACCEPTED ARTICLE

Disclaimer/Publisher's Note: The views expressed in this article are those of the author(s) and do not necessarily reflect the views of the publisher or editors. The publisher and editors assume no responsibility for any injury or damage resulting from the use of information contained herein.